JOURNAL OF SOLID STATE CHEMISTRY 48, 161–167 (1983)

The Intralayer Order–Disorder Transition in Monoclinic $Cr_{3\pm x}Se_4$

T. OHTANI*, R. FUJIMOTO, H. YOSHINAGA, AND M. NAKAHIRA†

Okayama University of Science, Laboratory for Solid State Chemistry, 1-1 Ridaicho, Okayama 700, Japan

AND Y. UEDA

Department of Chemistry, Faculty of Science, Kyoto University, Kyoto 606, Japan

Received November 29, 1982; in revised form January 25, 1983

The $Cr_{3\pm x}Se_4$ shows an order–disorder transition from the monoclinic Cr_3Se_4 type to the CdI_2-type structure. This transition originates in the intralayer disordering of metal vacancies in the alternate partially filled metal layers along the c axis. The transition is reversible and of first order. The transition temperature vs composition curve has a maximum (~900°C) at a stoichiometric composition of Cr_3Se_4. A statistical treatment of this phenomenon was attempted via the Bragg–Williams approximation.

Introduction

Many transition metal monochalcogenides (MX; M = metal, X = chalcogen) form the NiAs structure in which the chalcogens are hexagonally close packed and the metals occupy octahedral sites. In metal deficient compositions $M_{1-x}X$, the vacancies are distributed exclusively in alternate metal layers along the c axis.[1] When the alternate metal-vacancy layers are fully vacant, the compounds change to the MX_2 structure which coincides with the CdI_2 structure. In the MX and the MX_2 range, many vacancy-ordered phases exist which correspond to the different cation–anion ratios. Typical examples are given by the Cr–S and Cr–Se systems, which exhibit a great variety of possible vacancy-ordered phases, such as Cr_7X_8, Cr_5X_6, Cr_3X_4, Cr_2X_3 and Cr_5X_8 (*1–3*).

The compound $Cr_{3\pm x}Se_4$ has a monoclinic cell (I2/m) based upon the NiAs structure at room temperature, and shows a wide homogeneity range of $x \leq 0.20$ (*3, 4*). The arrangement of vacancies in the metal-vacancy layer is derived from the removal of Cr atoms from alternate rows of the full CrSe arrangement, which means that just one half of the lattice sites are vacant in metal-vacancy layers (see Fig. 6).

A few reports on the order–disorder transition have been published for the transition metal chalcogen systems (*5*). Recently Oka *et al.* reported successive intralayer order–disorder transitions in the VS_x and VSe_x systems ($1.30 \leq x \leq 1.70$), namely, V_5S_8-

* Author to whom correspondence should be addressed.

† Deceased.

[1] Hereafter, we describe this layer as the metal-vacancy layer.

0022-4596/83 $3.00

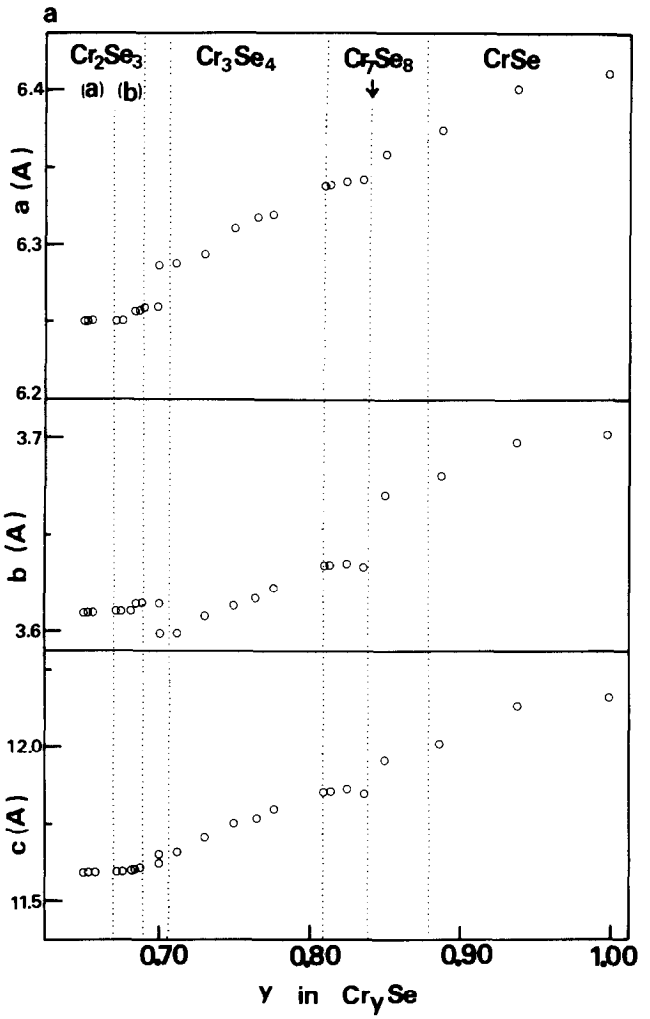

FIG. 1. Phase relationship of the Cr_ySe system ($0.65 \leq y \leq 1.0$) and the composition dependence of lattice parameters for specimens quenched from 600°C. The lattice parameters of the CrSe and Cr_2Se_3 phases are normalized to those of the Cr_3Se_4 phase. Cr_2Se_3 (a) and (b) has the rhombohedral and the trigonal structure, respectively (*7*, *8*).

type → V_3S_4-type → VS_2-type (CdI_2 structure) transitions on heating (*6*). They have qualitatively explained these phenomena by a statistical thermodynamic treatment.

In the present work we observed the intralayer order–disorder transition in $Cr_{3\pm x}Se_4$ (Cr_3Se_4-type to CdI_2-type on heating), the peak of the composition vs transition temperature curve being centered at a stoichiometric composition of Cr_3Se_4. A simple treatment based on the Bragg–Williams approximation was successfully used for interpreting this transition.

Experimental

Samples were prepared as follows. Pure Cr metal powder (99.9%) and Se (99.999%) were mixed in the appropriate ratios and pressed into pellets, followed by heating at 800°C in evacuated silica tubes for a week. After grinding, the samples were annealed

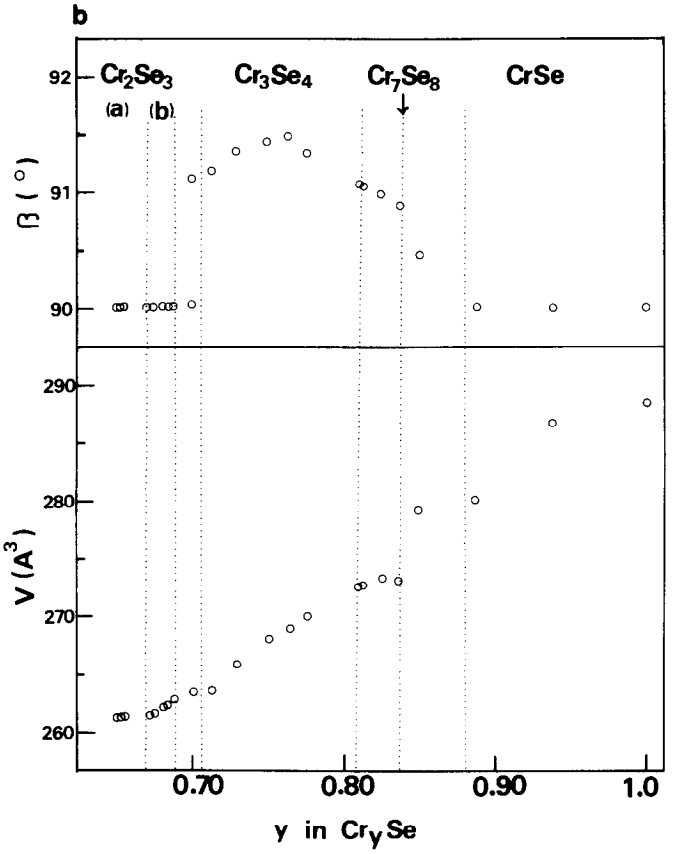

FIG. 1—*Continued.*

again at desired temperatures for two weeks and then quenched in water. A chemical analysis was performed by oxidizing the samples to Cr_2O_3 at 900°C in the air for 14 hr. The structure identification of quenched samples was carried out by the powder X-ray diffraction method. The lattice parameters were determined by the least-squares method using a computer. High-temperature X-ray diffraction measurements were taken at various temperatures up to 1100°C, using a commercial powder diffractometer specially designed for high-temperature measurements. The samples used for these measurements were sealed in evacuated silica capillaries. High-temperature DTA measurements were carried out from room temperature to 1100°C at a heating–cooling rate of 10°C/min for several samples which had been sealed in small silica capsules. Al_2O_3 was used as a reference.

Results and Discussion

In the present work, our interest was focused on the Cr_3Se_4 phase. We found it important to investigate the phase relationship between the neighbouring phases. We then prepared the compounds Cr_ySe with compositions between $y = 0.65$ and 1.00.

Figures 1(a) and (b) show the phase relationship close to the Cr_3Se_4 phase, and the composition dependence of lattice parame-

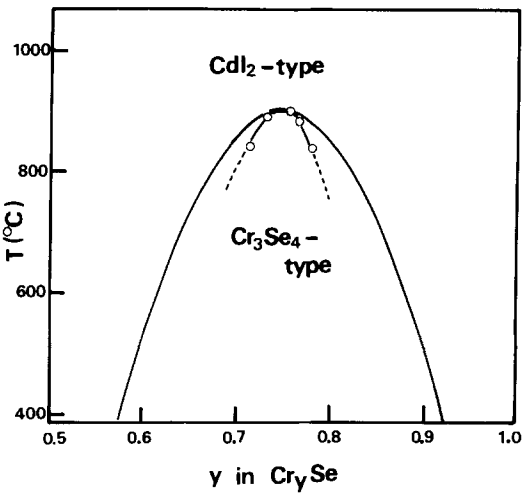

FIG. 2. Transition temperature vs composition curve for the Cr_3Se_4 phase. Experimental results obtained by DTA measurements are given by open circles. The parabolic solid line is a calculated result based on the Bragg–Williams approximation (see text).

ters for specimens quenched from 600°C. Lattice spacings of the CrSe and Cr_2Se_3 phases are normalized to those of the Cr_3Se_4-type cell. Here we mainly describe the Cr_3Se_4 phase. The homogeneity range of the Cr_3Se_4 phase at 600°C is $0.71 \leq y \leq 0.81$. The lattice constants (a, b, c, axis) of the Cr_3Se_4 phase continuously increase with decreasing vacancy. The unit cell volume also shows a similar behavior. On the other hand, the monoclinic angle β has a maximum close to the stoichiometric composition of Cr_3Se_4. A similar behavior has been observed in V_3S_4 (*9*) and V_3Se_4 (*10*) phases. These results would be correlated with the superstructure ordering which originates in the minimization of the repulsive interaction energy of vacancies. Hence it is plausible that the monoclinic distortion is most pronounced at the exact stoichiometric composition.

The most remarkable result found in this work is that the phase transition was observed in high-temperature DTA measurements in the Cr_3Se_4 phase. Experimental results are shown in Fig. 2 by open circles. The transition temperature (T_c) shows a parabolic change with composition, having a maximum at the stoichiometric composition. The maximum transition temperature is close to 900°C. The DTA profiles near the transition temperature are shown in Fig. 3 for $Cr_{0.73}Se$ ($Cr_{2.92}Se_4$). This transition is quite reversible for all compositions which were investigated, and exhibits a hysteresis. The hysteresis width is 6°C at the stoichiometric composition, and increases with the deviation from this composition. These results imply that the transition is of first order. The high temperature phase cannot be quenched to room temperature at any composition.

The crystal structure above T_c was determined by *in situ* observation, using high-temperature X-ray diffraction. The characteristic profiles of diffraction peaks and lattice parameters of $Cr_{0.73}Se$ ($Cr_{2.92}Se_4$) at different temperatures are shown in Figs. 4 and 5, respectively. With increasing temperature, the monoclinic structure becomes continuously less distorted, as seen in the temperature dependence of the peak pro-

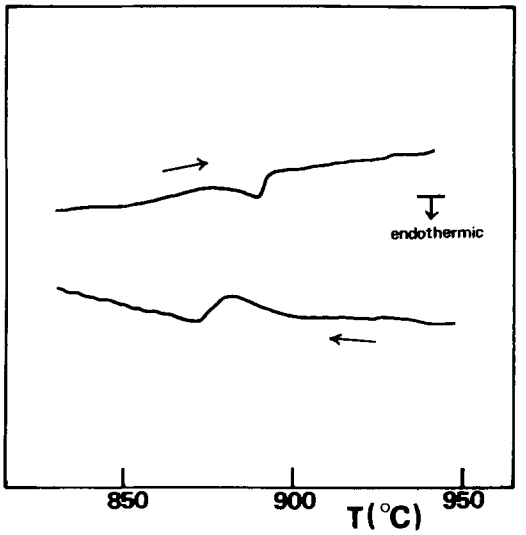

FIG. 3. DTA profiles of $Cr_{0.73}Se$ ($Cr_{2.92}Se_4$). Heating and cooling rates are 10°C/min.

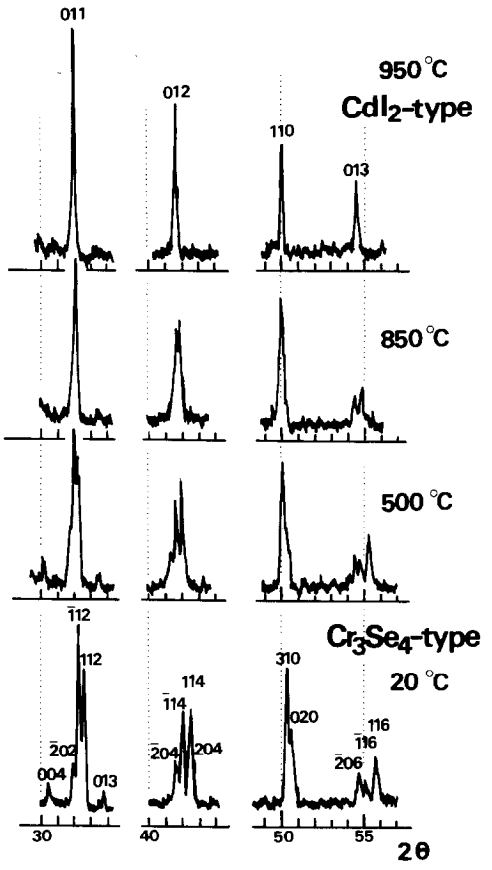

FIG. 4. Variation of characteristic X-ray diffraction peaks with temperature for $Cr_{0.73}Se$ ($Cr_{2.92}Se_4$).

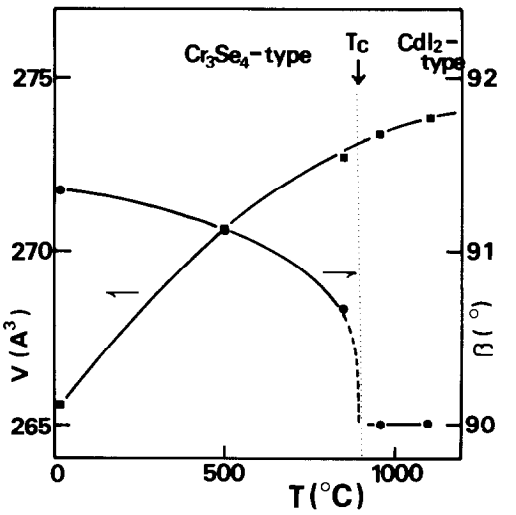

FIG. 5. Temperature dependence of the monoclinic angle β and the unit cell volume of $Cr_{0.73}Se$ ($Cr_{2.92}Se_4$). The unit cell volume of the CdI_2-type phase is normalized to that of the Cr_3Se_4-type structure.

files and of the monoclinic angle β. This is especially so at the temperature immediately below the transition, where the diffraction pattern is very close to that of the CdI_2 structure. Above the transition, the structure changes from the Cr_3Se_4-type to the CdI_2-type. The X-ray powder pattern of a NiAs-type structure is usually very similar to that of a CdI_2-type structure. However, one can exclude the possibility of the NiAs structure for the high-temperature phase, because 00l reflections with odd numbers of l were observed in the diffraction patterns. This result is easily understandable from the thermodynamic point of view which predicts that the transition to the NiAs structure is expected to occur at even more elevated temperatures (*6*). Furthermore, in diffraction patterns above the transition there is no evidence to show any extra peak which would be responsible for the superstructure formation. It is thus likely that the transition is of the intralayer order–disorder type, where metal vacancies in the alternate metal-vacancy layers take on a disordered arrangement above T_c. As mentioned before, the transition is of first order. Nevertheless, from the continuous change of unit cell volume with temperature as shown in Fig. 5, this transition seems to be close to second order.

The transition may be regarded as a two-dimensional order–disorder type. Thus, we can treat this transition by using the simple Bragg–Williams approximation. We take the Cr_3Se_4-type structure as the basic structure. In Fig. 6, the crystal structure of Cr_3Se_4-type is depicted with the sulfur atoms omitted. For simplicity, the lattice is assumed to be pseudo-hexagonal because the monoclinic angle β is close to 90°. We designate the metal sites as A, B, and C as shown in Fig. 6. When the occupation prob-

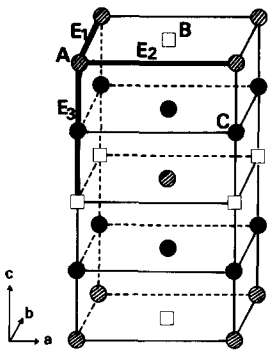

FIG. 6. Schematic crystal structure of monoclinic Cr_3Se_4. The selenium atoms have been eliminated for simplicity. The closed and shaded circles are Cr metal atoms at C and A sites, respectively, while the open circles represent vacancies at the B site. E_1, E_2, and E_3 are pairwise interaction energies (see text).

abilities are expressed as x_A, x_B, and x_C for A, B, and C sites, respectively, the following expression is expected for each structure; $x_A = x_C = 1$, $x_B = 0$ for the Cr_3Se_4-type structure, $x_A = x_B < 1$ ($= \frac{1}{2}$ at the stoichiometry of Cr_3Se_4), $x_C = 1$ for the CdI_2-type structure.

Next, we construct the free energy expression in a way similar to that reported by Koiwa and Hirabayashi (*11*), who investigated the order–disorder transition of oxygen atoms in Ti–O system. Adopting the Bragg–Williams approximation for the estimation of the interaction energy between Cr atoms in the metal-vacancy layers, the configurational energy is expressed as follows:

$$E = \frac{1}{2} N_A\left(2N_A\Big/\frac{N}{4} + 4N_B\Big/\frac{N}{4}\right)(E_1 + E_2) + \frac{1}{2} N_B\left(2N_B\Big/\frac{N}{4} + 4N_A\Big/\frac{N}{4}\right)(E_1 + E_2) + \frac{1}{2}\left(N_A N_B\Big/\frac{N}{4}\right)E_3, \quad (1)$$

where N is the total number of Cr atoms, and N_A and N_B are the number of Cr atoms on A and B sites, respectively. E_1 and E_2 are the pairwise interaction energies between nearest neighbors and second nearest neighbors in the metal-vacancy layers, respectively. E_3 is the interlayer pairwise interaction energy between neighboring metal-vacancy layers. E_1, E_2, and E_3 are depicted in Fig. 6.

On counting the number of ways of arranging atoms on A and B sites, the configurational entropy S is obtained by using the Stirling approximation as follows,

$$S = -\frac{N}{4} k \ln \frac{\left(\frac{N}{4}\right)!}{N_A!\left(\frac{N}{4} - N_A\right)!} \cdot \ln \frac{\left(\frac{N}{4}\right)!}{N_B!\left(\frac{N}{4} - N_B\right)!}$$

$$\doteqdot -\frac{N}{4} k \left[\left\{N_A \ln \frac{\frac{N}{4}}{N_A} + \left(\frac{N}{4} - N_A\right)\ln \frac{\frac{N}{4}}{\frac{N}{4} - N_A}\right\} + \left\{N_B \ln \frac{\frac{N}{4}}{N_B} + \left(\frac{N}{4} - N_B\right) \ln \frac{\frac{N}{4}}{\frac{N}{4} - N_B}\right\}\right]. \quad (2)$$

When using the occupation probabilities $x_A = N_A/(N/4)$ and $x_B = N_B/(N/4)$ instead of the numbers of the Cr atoms, the free energy is given by the following equation:

$$G = \frac{N}{4}\left[\{(x_A^2 + 4x_A x_B + x_B^2)(E_1 + E_2) + 2x_A x_B E_3\} + kT\{x_A \ln x_A + (1 - x_A) \ln (1 - x_A) + x_B \ln x_B + (1 - x_B) \ln (1 - x_B)\}\right]. \quad (3)$$

To obtain the critical temperature (T_c), it is convenient to express Eq. (3) as a function of a long-range order parameter s, which can be characterized as follows:

$$N_A = (2y - 1)(1 + s)N/4 = x_A \cdot N/4,$$
$$N_B = (2y - 1)(1 - s)N/4 = x_B \cdot N/4, \quad (4)$$

where y is the composition of the Cr atoms in the expression Cr_ySe. The critical temperature T_c is given by minimizing the free energy with respect to s. The condition for determining T_c is therefore

$$s = 0 \qquad \left(\frac{\partial F(s)}{\partial s}\right)_{s=0} = 0$$
$$\left(\frac{\partial^2 F(s)}{\partial s^2}\right)_{s=0} = 0. \quad (5)$$

Solving these equations, T_c is obtained as

$$T_c = \frac{4(E_1 + E_2 + E_3)}{k}(2y - 1)(1 - y). \quad (6)$$

The calculated results are compared with experimental results in Fig. 2. Considering the rough approximation in the present treatment, the experimental results are rather well fitted to the calculation. A higher degree of approximation is required for obtaining improved coincidence between experiments and theory.

In conclusion, we observed the intralayer order–disorder transition of vacancies in the $Cr_{3\pm x}Se_4$ system. The transition temperature vs composition curve has a maximum (~900°C) at the stoichiometric composition, and can be qualitatively explained by a simple treatment based on the Bragg–Williams approximation.

Acknowledgments

The authors express their sincere thanks to Professor S. Kachi and Professor K. Kosuge for reading of the manuscript and for many fruitful discussions.

References

1. F. JELLINEK, *Acta Crystallogr.* **10,** 620 (1957).
2. H. HARALDSEN AND F. MEHMED, *Z. Anorg. Allg. Chem.* **239,** 369 (1938).
3. M. CHEVRETON, *Bull. Soc. Fr. Mineral. Cristallogr.* **90,** 592 (1967).
4. M. CHEVRETON AND F. BERTAUT, *C.R. Acad. Sci.* **253,** 145 (1961).
5. C. F. VAN BRUGGEN AND F. JELLINEK, "Propr. Thermodyn. Phys. Struct. Dériv. Semi-Métal.," p. 31, CNRS, Paris (1967); H. PLOVNICK, D. S. PERLOFF, M. VLASSE, AND A. WOLD, *J. Phys. Chem. Solids* **29,** 1935 (1968); T. J. A. POPMA AND C. F. VAN BRUGGEN, *J. Inorg. Nucl. Chem.* **31,** 73 (1969); H. NAKAZAWA, M. SAEKI, AND M. NAKAHIRA, *J. Less-Common Metals* **44,** 341 (1976).
6. Y. OKA, K. KOSUGE, AND S. KACHI, *J. Solid State Chem.* **23,** 11 (1978); **24,** 41 (1978).
7. M. CHEVRETON AND B. DUMONT, *C.R. Acad. Sci. Ser. C.* **267,** 884 (1968).
8. F. H. WEHMEIER, E. T. KEVE, AND S. C. ABRAHAMS, *Inorg. Chem.* **9,** 2125 (1970).
9. M. NAKANO-ONODA AND M. NAKAHIRA, *J. Solid State Chem.* **30,** 283 (1979).
10. K. MIYAUCHI, private communication.
11. M. KOIWA AND M. HIRABAYASHI, *J. Phys. Soc. Jpn.* **27,** 807 (1969).